

Shahid Chamran
University of AhvazIranian Association of
Electrical and Electronics
Engineers

Journal of Applied Research in Electrical Engineering

E-ISSN: 2783-2864

P-ISSN: 2717-414X

Homepage: <https://jaree.scu.ac.ir/>

Research Article

Improving the Performance Characteristics of Conventional Linear Switched Reluctance Motor by Eliminating Translator Yoke and Embedding Permanent Magnets in Stator Yoke

Milad Golzarzadeh^{1,*} , Hashem Oraee¹ , and Babak Ganji² 

¹ Department of Electrical Engineering, Sharif University of Technology, Tehran, Iran

² Faculty of Electrical and Computer Engineering, University of Kashan, Kashan, Iran

* Corresponding Author: milad.golzarzadeh@ee.sharif.edu

Abstract: In this paper, the Segmental Translator Permanent Magnet Linear Switched Reluctance Motor (STPMLSRM) has been introduced as a new type of improved Linear Switched Reluctance Motor (LSRM), which increases the flux density in the air-gap by using Permanent Magnets (PMs) in the stator yoke. Also, the moving part does not have a yoke, and discrete segments are used instead of the yoke, which reduces the volume of active magnetic materials. In order to better evaluate, the segmental translator permanent magnet linear switched reluctance motor is compared with the conventional linear switched reluctance motor and Segmental Translator Linear Switched Reluctance Motor (STLSRM) without permanent magnet, then their different aspects are discussed. In order to validate the introduced STPMLSRM, based on the Finite Element Method (FEM), the static and dynamic characteristics of linear motors including static flux-linkage, static force, co-energy, instantaneous current waveform, and instantaneous thrust waveform are predicted and compared. These comparisons show that the STPMLSRM has better performance characteristics than the conventional LSRM and STLSRM.

Keywords: Linear switched reluctance motor, segmental translator, permanent magnet, finite element method.

Article history

Received 10 March 2024; Revised 27 June 2024; Accepted 17 October 2024; Published online 20 April 2025.

© 2025 Published by Shahid Chamran University of Ahvaz & Iranian Association of Electrical and Electronics Engineers (IAEEE)

How to cite this article

M. Golzarzadeh, H. Oraee, and B. Ganji, "Improving the performance characteristics of conventional linear switched reluctance motor by eliminating translator yoke and embedding permanent magnets in stator yoke," *J. Appl. Res. Electr. Eng.*, vol. 3, no. 2, pp. 222-231, 2024. DOI: [10.22055/jaree.2024.46343.1111](https://doi.org/10.22055/jaree.2024.46343.1111)



1. INTRODUCTION

Switched Reluctance Motors (SRMs) have advantages such as simplicity of structure, robustness, no magnet or winding on one side and high fault tolerance, which makes them a suitable choice for many applications [1-3]. Linear switched reluctance motors have a structure similar to rotary SRMs, with the difference that the movement is linear instead of rotary and linear force is produced instead of torque. Therefore, they have all the advantages of SRM. These motors are widely used in applications such as transportation systems, home use, and etc. [4-6]. Electric trains and elevators are other applications of LSRMs [7, 8]. In these motors, both distributed windings and centralized windings are used, which can be mechanically and electrically isolated, so they have high reliability. These windings are placed in the stator or mover. Structures in which the winding is located on the translator produce more force than the structure in which the winding is located on the stator. In addition, the cost of mass production of these systems is lower [9-11].

In order to improve the performance of SRM and reduce its disadvantages, various structures have been presented, in most of which the structure complexity has increased and their production has also become more difficult. Considering that the principles and performance of LSRM are similar to the rotary SRM, the methods of improving the performance of rotary SRM can be used to improve the performance characteristics of LSRM. One of the ways to improve the performance of LSRM is to remove the yoke in stator or translator, where by using independent segments, the thrust force of new motor increases compared to conventional motors. This method is used both in rotary SRMs [12-14] and in linear SRMs [15-17], which significantly improves the performance characteristics of motor. Another way to improve the performance of LSRM is to use permanent magnet (PM) in the stator or translator, which creates a new structure. Choosing the right location for PMs in the motor is very important. By choosing an inappropriate location, some of the advantages of LSRM such as simplicity of structure,

reliability and endurance are lost [18-20]. In [21], by using the PM in structure of LSRM and linear flux switching motor, a comparison has been made between these two motors. This comparison shows that using the PM in the LSRM structure gives a better result. In [22], two improved double-sided LSRMs with PMs embedded in their structure are introduced. By comparing both structures, it is shown that using the PM in the structure of motors, the flux density in the air-gap has increased, which leads to a decrease in the magnetic saturation and an increase in thrust force of the motor. In these two structures, due to the fact that PMs are located in the mover, the reliability of motors may decrease due to the movement of PMs.

The segmental translator linear switched reluctance motor (STLSRM) is one of the structures whose performance characteristics are improved compared to the conventional LSRM. Although the STLSRM has better performance than the conventional LSRM, few research has been carried out to introduce this motor. Also, in recent studies for the STLSRM, a model that uses the PM in its structure has not been presented. In [23], different structures of linear switched reluctance motor have been investigated and their static and dynamic characteristics have been compared based on the finite element method. In this paper, with the aim of improving the results presented in [23], changes including how to choose the right location for embedding permanent magnets in the motor structure, more detailed comparisons of the results, providing more details about the parameters and calculating specific parameters such as the average instantaneous power for different structures have been applied. Therefore, in this paper, in order to show the advantages of STPLSRM compared to the conventional LSRM and STLSRM, firstly, a comparison is made between these motors, then, by placing PMs in the stator yoke of STLSTM, the segmental translator permanent magnet linear switched reluctance motor (STPMLSRM) is presented as a new structure. In order to show the effect of PMs on motors, the performance characteristics of STLSRM and STPMLSRM are predicted and compared. The novelties of this paper are the use of discrete segments instead of poles connected to the yoke in the moving part and adding PMs in the stator yoke. In this structure, compared to conventional LSRM, less magnetic material is used, and due to the presence of PMs, the flux density in the air-gap increases significantly, which causes more thrust force to be applied to the moving part. Based on this, modeling of motors and their comparison is carried out in Section 2 and the simulation results are presented in Section 3. Finally, the conclusion is given in Section 4.

2. DIFFERENT STRUCTURES OF LSRM

2.1. Conventional Linear Switched Reluctance Motor

The cross-section of a conventional LSRM is shown in Fig. 1. As it is clear from this figure, each stator slot is filled with the windings of two phases, and two windings that are connected in series form one phase. There are no coils or permanent magnets in the moving part (translator), which makes it electrically isolated and increases reliability. This motor (Fig. 1) is like a 6/4 rotary switched reluctance motor,

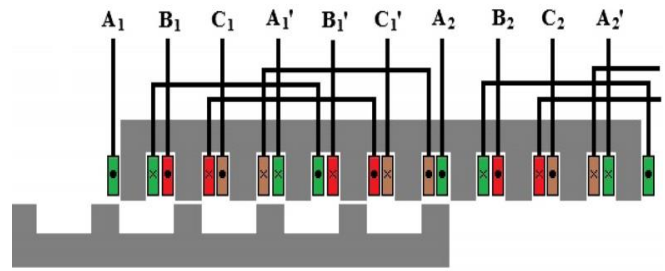


Fig. 1: 2-D geometry of conventional LSRM [15].

with extra poles in the stator and translator to reduce noise and end effect. These poles are connected by a yoke to create a flux path. The presence of a yoke in the motor body significantly increases the use of magnetic materials, which increases iron loss and reduces the force applied to translator [15].

2.2. Segmental Translator Linear Switched Reluctance Motor

The cross-section of a STLSRM is shown in Fig. 2. Each unit of this motor includes six poles and six slots in the stator and four segments in the translator. Therefore, in any length of this motor, the ratio of the number of stator poles to the translator segments is 3/2. To create a flux path in stator, the poles are connected by a yoke, while there is no yoke in the translator and instead of prominent poles, discrete segments are used. The segments are magnetically and mechanically independent from each other, and there is air or non-magnetic material between them. Since, the yoke has a considerable volume and weight of active magnetic materials, the use of magnetic materials in this motor is significantly reduced. The lack of yoke and special structure of translator makes the STLSRM produce more power than the conventional LSRM [16].

The STLSRM consists of three phases, each phase includes three stator poles. The current direction of coils enters from the first three slots and exits from the second three slots. According to Fig. 2, each phase occupies two slots of stator, and each slot of stator is filled only with the windings of one phase. Due to the type of placement of coils, the windings of different phases are mechanically independent from each other and no insulation is needed to separate the windings in the slots. Therefore, when one winding is damaged, the faulty winding can be replaced without damaging the other windings [17].

The prominent advantages of the STLSRM compared to the conventional LSRM are stated as follows:

- Only one coil is placed in each slot. Therefore, the use of insulating materials in the stator slot decreases and its space coefficient increases, which increases the output power.
- Optimum use of the stator slot surface and simplification of the manufacturing process due to the absence of an insulating separator in the stator slot.
- Due to the special structure of translator, the flux produced by each phase is independent from other phases.

- The translator does not have a yoke. Therefore, the use of magnetic materials is significantly reduced.
- Due to the fact that there is no pole or slot in the secondary, the windage loss in the translator is zero.
- Due to the absence of a yoke in the translator and the use of less iron, iron losses are reduced.

2.3. Segmental Translator Permanent Magnet Linear Switched Reluctance Motor

The use of PMs in the STLSRM makes a new structure that is effective in improving the performance of this motor. In recent studies for the STLSRM, a model that uses a PM in its structure has not been presented. Therefore, here by embedding the PMs in the motor body, the segmental translator permanent magnet linear switched reluctance motor (STPMLSRM) is presented as a new structure. The main role of the PM is to increase the flux density in air-gap, which reduces the magnetic saturation in the iron parts and the average current. Also, adding the PMs in the motor structure causes the motor produce more thrust force. For a better evaluation, the STLSRM of Fig. 2, is considered, in which there are no PMs in its structure and only phase (B) is excited. With simulation based on 3-D FEM and using ANSYS-Maxwell software, flux density distribution and magnetic flux path are obtained for the motor structure without PMs, which are shown in Fig. 3. In this case, by passing the magnetic flux through the teeth around the coil, air-gap and translator segments, the force is applied to the motor translator. The average static force for a current 10 A and different positions of the translator is equal to 108 N.

To investigate the effect of PMs on flux density distribution and magnetic flux path in the STPMLSRM, firstly, it is assumed that current of phase B is zero and only PMs create magnetic flux. For this purpose, PMs are placed in the stator yoke, then the motor is simulated and their results are discussed. Using modeling based on the FEM, flux density distribution and magnetic flux path are obtained according to Fig. 4. This figure shows that with the presence of PMs in the motor stator yoke and zero excitation current, a significant part of the magnetic flux lines produced by the PMs, close their path through the iron core with very low reluctance, the air-gap with high reluctance and the translator segments, which causes the force to be applied to translator.

Embedding PMs in the translator causes the PMs to move with the moving part, which challenges the outstanding advantages of the SRM by considering the mechanical factors. Therefore, PMs are embedded in the stator. The location of PMs in the stator should be in such a way that the flux produced by them and the flux produced by the coils are in the same direction to increase the flux density in the air-gap. In addition, the PMs should be placed in such a way that they completely cover the flux path produced by the coils. Therefore, the stator yoke section above the stator slot is a suitable location. Due to the fact that in this structure, the PM completely blocks the stator yoke, most of the flux produced by the PMs inevitably passes through the air-gap between the stator and translator, which increases the air-gap flux density. In the full load condition, where both the PMs and the winding of phase B generate magnetic flux, as shown in Fig. 5, the flux generated by PMs is in the same direction as the flux generated by phase B, which increases the flux density

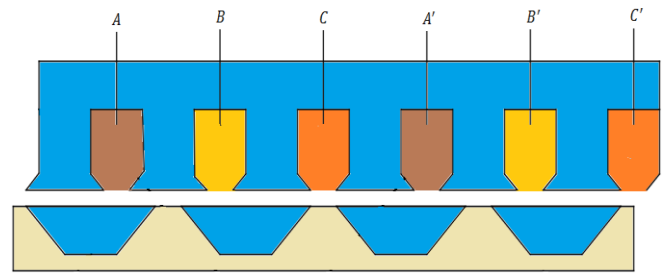


Fig. 2: Two-dimensional geometry of STLSRM.

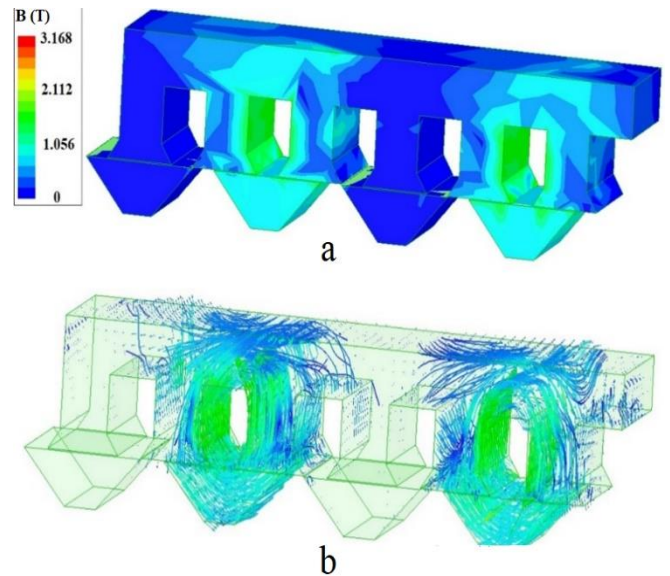


Fig. 3: Modeling of STLSRM without PM for current 10 A: (a) Flux density distribution, (b) Magnetic flux path.

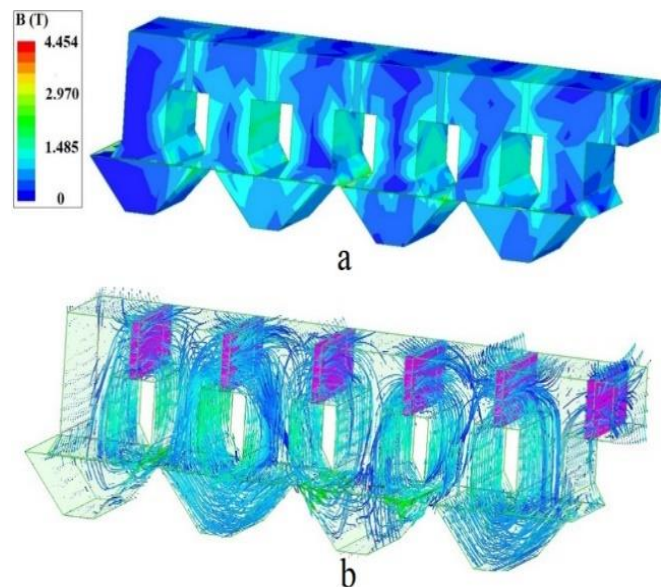


Fig. 4: Modeling of STLSRM by embedding PMs in the yoke and current 0 A: (a) Flux density distribution, (b) Magnetic flux path.

in air-gap, and in this case, the force applied to the translator is strengthened and the motor performance is improved. For different positions of translator (0 - 69 mm) and a current of 10 A, the average static force in the presence of PMs is equal to 195 N, which is more than the STLSRM without PM.

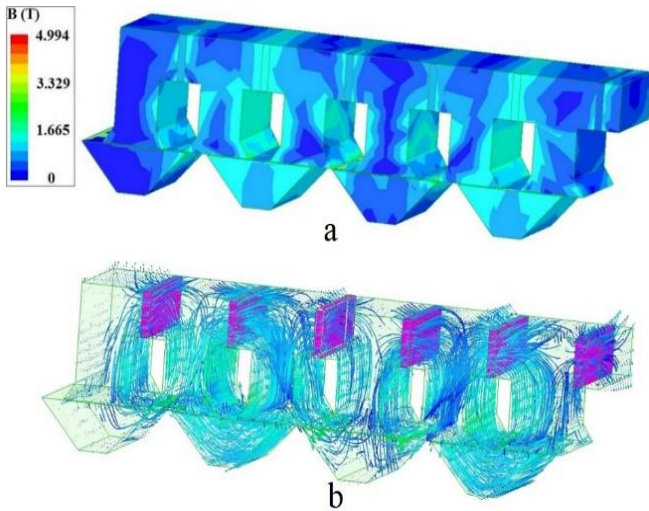


Fig. 5: Modeling of STL SRM by embedding PMs in the yoke and current 10 A: (a) Flux density distribution, (b) Magnetic flux path.

3. SIMULATION RESULTS

The simulation results for different topologies of linear switched reluctance motor based on the FEM are given here and compared. The specifications of motors are given in Tables 1 and 2, and the stator and translator core sheets are M800-50A with a thickness of 0.5 mm. The LSRMs generate thrust force by changing reluctance. The power produced of these motors is created by the co-energy difference between the fully aligned and fully unaligned positions. The flux path in two important positions for STL SRM and conventional LSRM are shown in Fig. 6 and Fig. 7, respectively. As can be seen in Fig. 6, in the aligned position, two poles adjacent in the stator pass the flux, while in the conventional LSRM as shown in Fig. 7, only one stator pole passes the flux. Therefore, it is clear that the proposed STL SRM can carry more flux.

Based on the 2-D FEM, the flux-linkage with a phase is calculated for the STL SRM and the conventional LSRM in different positions (0 - 69 mm) and shown in Fig. 8. For a better evaluation, the flux-linkage of STL SRM and the conventional LSRM are compared for two important positions including fully aligned and fully unaligned in Fig. 9 and Table 3. As can be seen in this figure, the co-energy difference between the two critical positions in the STL SRM is greater than that of the conventional LSRM.

Using the static characteristic of Flux-linkage, the co-energy characteristic is obtained from the following equation:

$$w_c(x, i) = \int \lambda(x, i) di \tag{1}$$

The co-energy characteristic in the current range of 0 to 20 A for two motors is shown in Fig. 10. This figure clearly shows that the co-energy difference in the STL SRM is higher than the conventional LSRM. Therefore, the STL SRM produces more static force at equal current.

The characteristic of static force ($F(x, i)$) is predicted from the following equation:

$$F(x, i) = \frac{\partial w_c(x, i)}{\partial x} \Big|_{i=\text{const}} \tag{2}$$

Table 1: Specifications of STL SRM.

Parameter	Value
Stator pole width [mm]	46
Stator slot width [mm]	46
Stator pole height [mm]	67
Stator core depth [mm]	46
Air-gap length [mm]	1
Segment width [mm]	115
Slot opening width [mm]	23
Segment height [mm]	46
Core stack thickness [mm]	125
Turns per phase	160

Table 2: Specifications of conventional LSRM.

Parameter	Value
Stator pole width [mm]	46
Stator slot width [mm]	46
Stator pole height [mm]	67
Stator yoke height [mm]	46
Air-gap length [mm]	1
Translator pole width [mm]	49
Translator slot width [mm]	89
Translator yoke height [mm]	49
Core stack thickness [mm]	125
Turns per phase	160

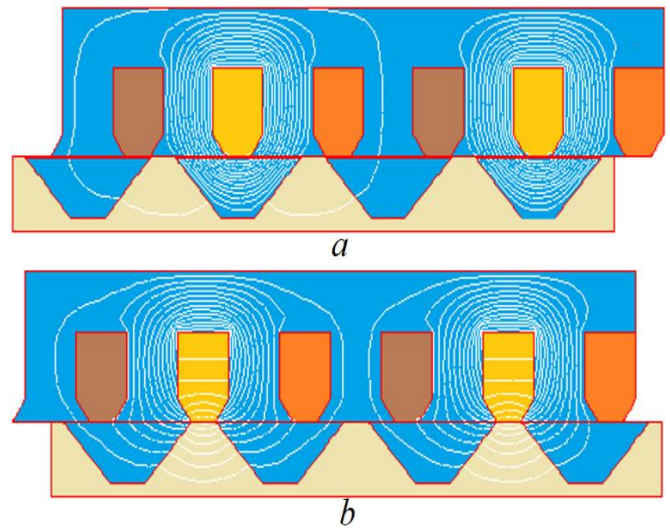


Fig. 6: Important positions for STL SRM (a) Aligned position, (b) Unaligned position.

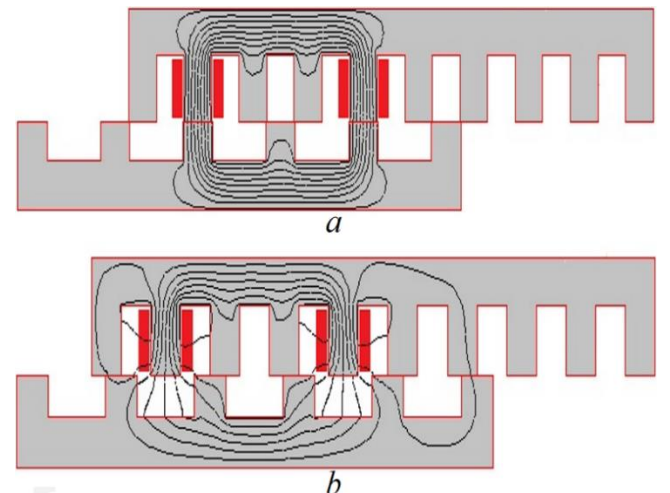


Fig. 7: Important positions for conventional LSRM, (a) Aligned position, (b) Unaligned position.

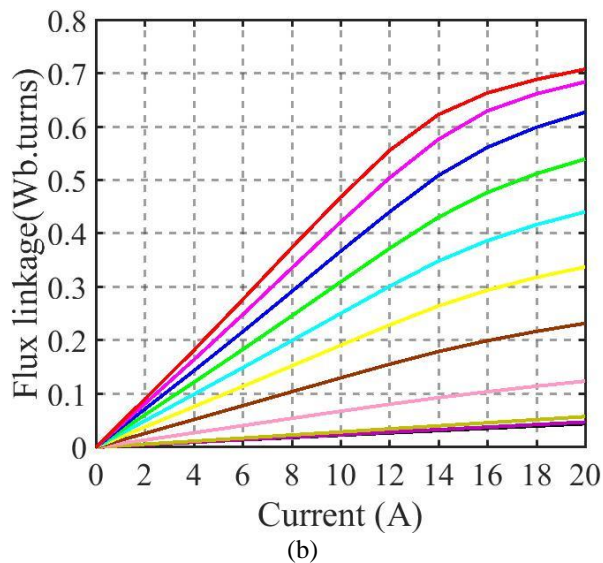
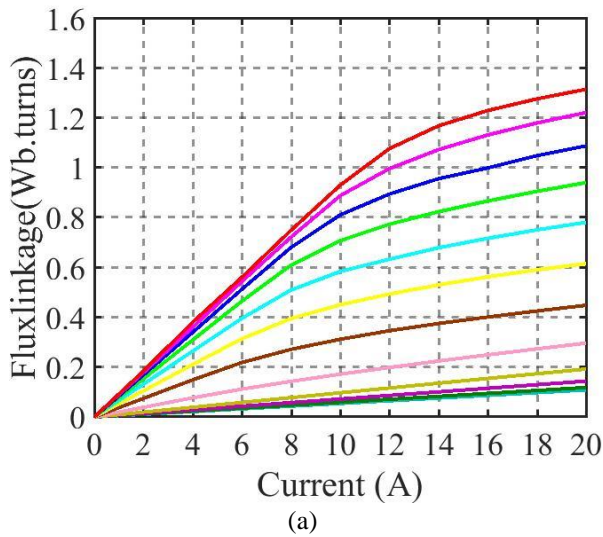


Fig. 8: Flux-linkage with a phase: (a) STLSRM, (b) conventional LSRM.

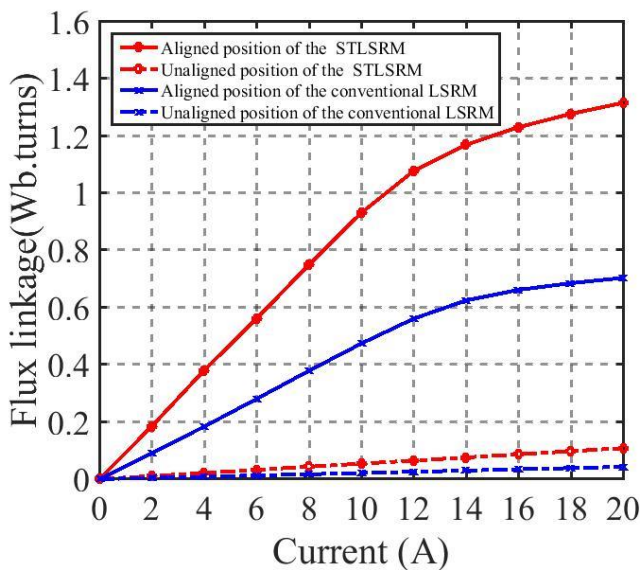


Fig. 9: Flux-linkage for two important positions.

Table 3: The values of flux-linkage (Wb.turns) predicted for two positions.

Position	Motor type	Current (A)			
		2	6	10	14
Unaligned	LSRM	0.004	0.013	0.022	0.030
	STLSRM	0.011	0.033	0.054	0.076
Aligned	LSRM	0.091	0.280	0.474	0.625
	STLSRM	0.184	0.561	0.931	1.170

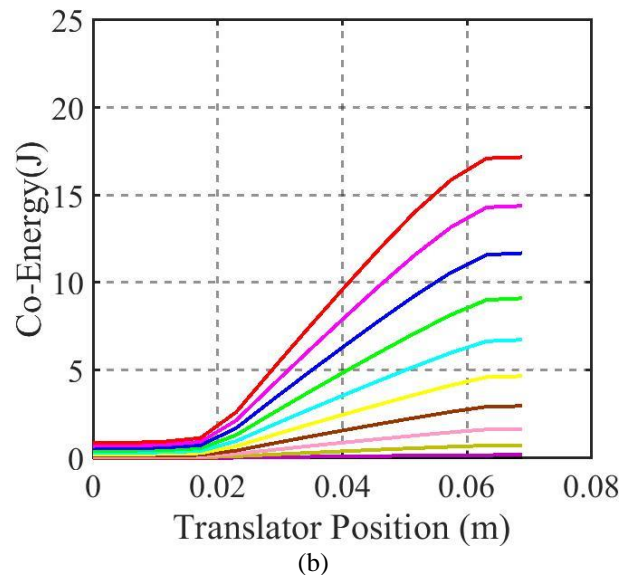
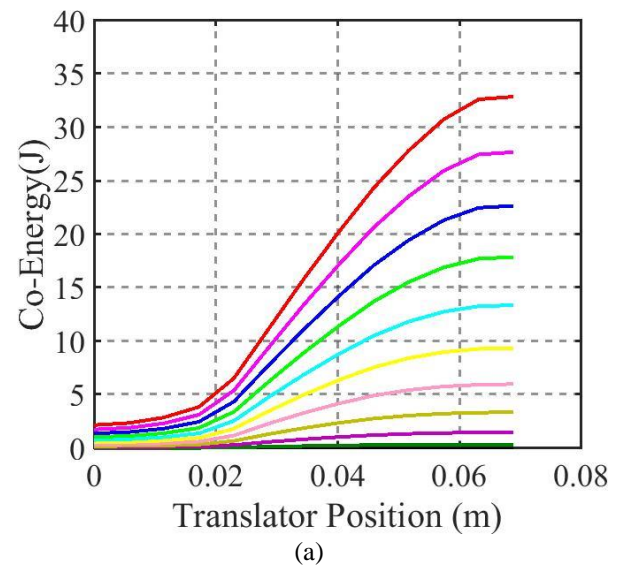


Fig. 10: The co-energy characteristic: (a) STLSRM, (b) conventional LSRM.

For STLSRM and conventional LSRM, the static force characteristics in terms of translator positions are obtained by solving (2) and shown in Fig. 11. For better evaluation, the average static force in terms of different currents for two motors are calculated and compared in Fig. 12 and Table 4,

which shows that the STLSRM produces more force than the conventional LSRM. For a better comparison of motors, instantaneous current ($i(x)$) and instantaneous thrust force ($F(x)$) can be used. The instantaneous current is predicted from the phase voltage equation of the SRM as follows:

$$V = Ri + \frac{d\lambda(x, i)}{dt} \tag{3}$$

where R is the resistance of the phase winding and V is the phase voltage. Having $i(x)$ and $F(x, i)$, $F(x)$ is calculated. Therefore, the dynamic characteristics of motors, including instantaneous current and instantaneous thrust force, for the working point: speed = 4 m/s, turn-on position = 15.8 (mm), turn-off position = 28.3 (mm) and the current regulation control mode when maximum current is 7 A, are predicted and compared in Fig. 13. It should be noted that in Fig. 10 and 11 obtained from equations (1) and (2), each color shows a current from 2 to 20 A.

The average instantaneous thrust force for STLSRM and conventional LSRM are 61.22 N and 32.18 N, respectively, while, the effective value of instantaneous phase current for STLSRM and conventional LSRM are 5.18 A and 7.28 A, respectively, which shows that with less effective current, more average thrust force is obtained for the STLSRM. The output power of the linear motor is calculated from $P_o = F_{tr}V_m$. In this equation, F_{tr} is the thrust force of translator and V_m is the linear velocity of translator. Therefore, using the dynamic characteristic of instantaneous thrust force (Fig. 13), the average instantaneous power for two motors is calculated. The average instantaneous power for STLSRM and the conventional LSRM are 244.4 W and 128.72 W, respectively, which shows that the average power for STLSRM is more than conventional LSRM.

In order to compare the performance of STLSRM and STPMLSRM, simulation results are given based on 3-D FEM and PMs are NdFeB35 with $\mu_r = 1.09$ and $B_r = 1.23$ T. The flux-linkage static characteristics of one phase for two motors are predicted and shown in Fig. 14. This figure has been obtained by applying currents of 0 to 16 A to the phase B and by moving from unaligned position to aligned position with a length of 69 mm. For a better evaluation, the flux-linkage of motors are compared for only two important positions including fully aligned and fully unaligned in Fig. 15 and Table 5. In this figure, the effect of PM is clearly visible. In the STLSRM, when there is no excitation current, the flux-linkage is zero both in the aligned and unaligned positions, but in the STPMLSRM with zero excitation current, the flux-linkage is greater than zero in all positions of translator. It should be noted that in Fig 8 and 14, which are the graphs of flux-linkage in terms of current, each color shows a position of the translator from the fully unaligned position to the fully aligned position.

The co-energy difference between the aligned and unaligned positions for the STPMLSRM is greater than the STLSRM, since the area between the flux-linkage in the aligned and unaligned positions is greater for the PM motor than for the motor without PM. Therefore, adding the PM in the motor structure increases the force applied to the translator. The average static force at different currents for two motors has been calculated using the static force characteristics, which are compared in Fig. 16 and Table 6.

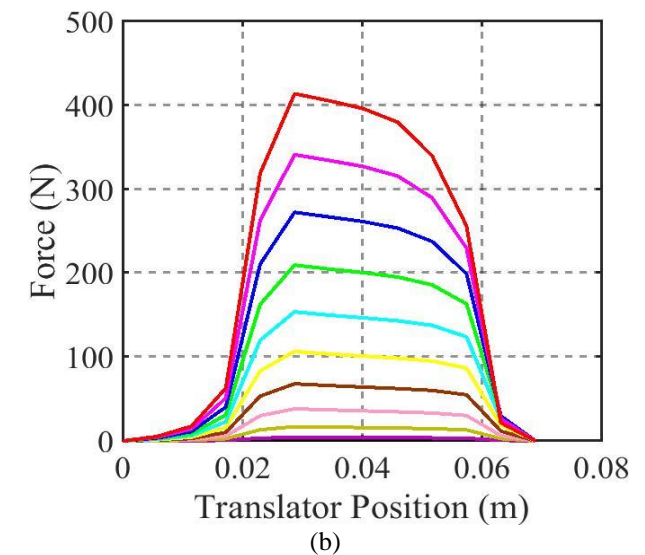
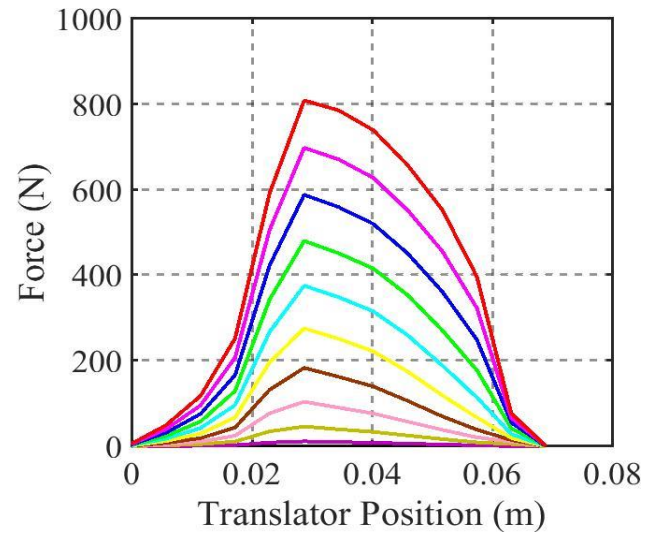


Fig. 11: The static force characteristics: (a) STLSRM, (b) conventional LSRM.

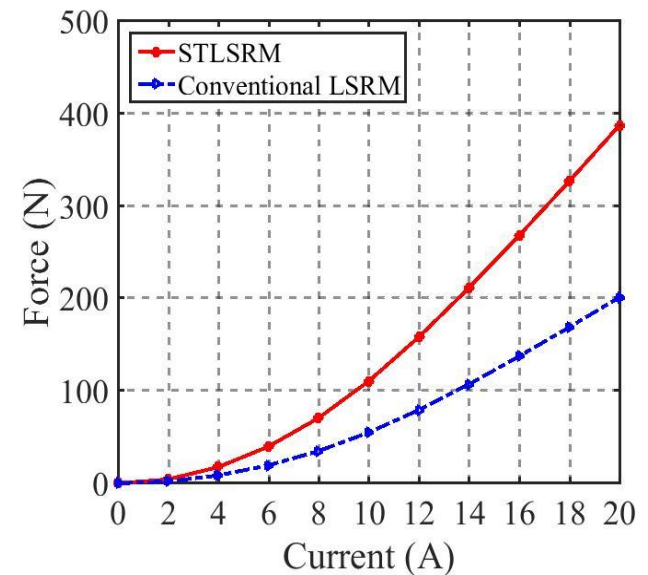


Fig. 12: Average static force for two linear motors.

Table 4: Average static force (N) of conventional LSRM and STL SRM for different currents.

Current (A)	Average force for LSRM	Average force for STL SRM
2	2.1	4.3
4	8.6	17.6
6	19.5	39.7
8	34.9	70.7
10	55	110.5
12	79.3	158.2
14	107.2	211.5
16	137.4	268.1
18	168.9	326.8
20	201.3	387.2

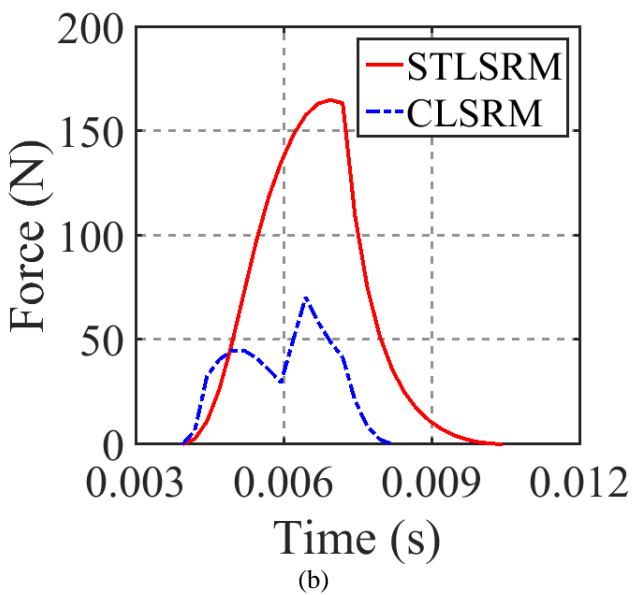
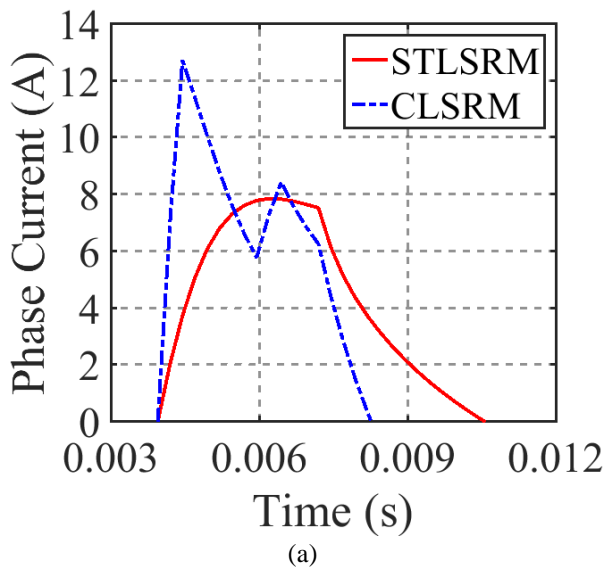


Fig. 13: Dynamic waveforms: (a) Instantaneous phase current, (b) Instantaneous thrust force.

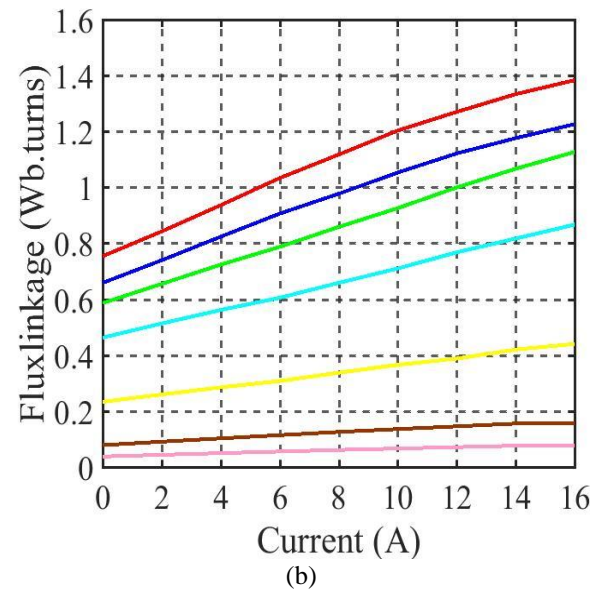
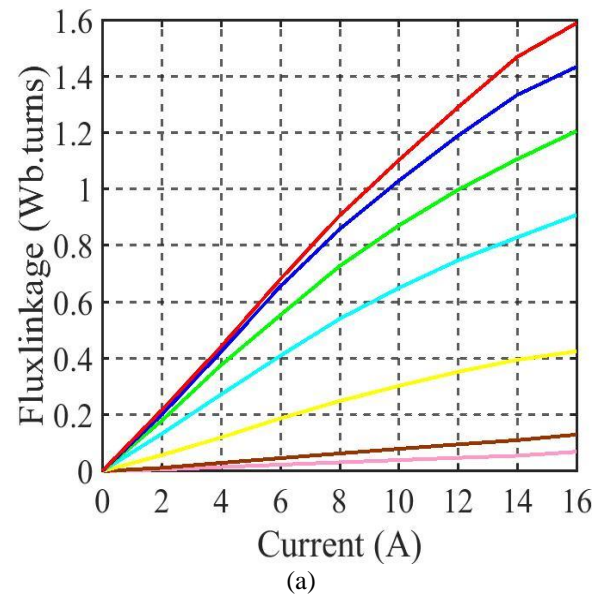


Fig. 14: 3-D Flux-linkage with a phase: (a) STL SRM, (b) STPML SRM.

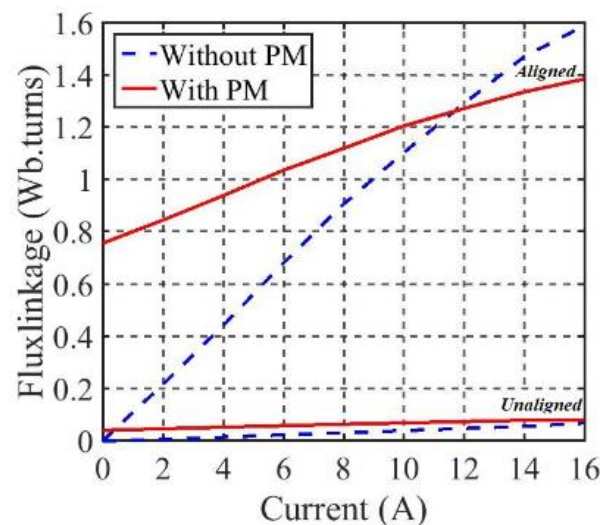


Fig. 15: Flux-linkage for positions of fully aligned and fully unaligned.

Table 5: The values of flux-linkage (Wb.turns) predicted for aligned and unaligned positions.

Position	Motor type	Current (A)			
		2	6	10	14
Unaligned	STPMLSRM	0.047	0.059	0.069	0.079
	STLSRM	0.006	0.023	0.040	0.055
Aligned	STPMLSRM	0.846	1.036	1.206	1.337
	STLSRM	0.230	0.714	1.124	1.519

Table 6: Average static force (N) of STLSRM and STPMLSRM for different currents.

Current (A)	Average force for STLSRM	Average force for STPMLSRM
2	4.7	32.9
4	19	69.7
6	43.3	110.7
8	77.6	155.6
10	120.9	203.9
12	172.7	255.1
14	233.1	308.7
16	299.9	364.2

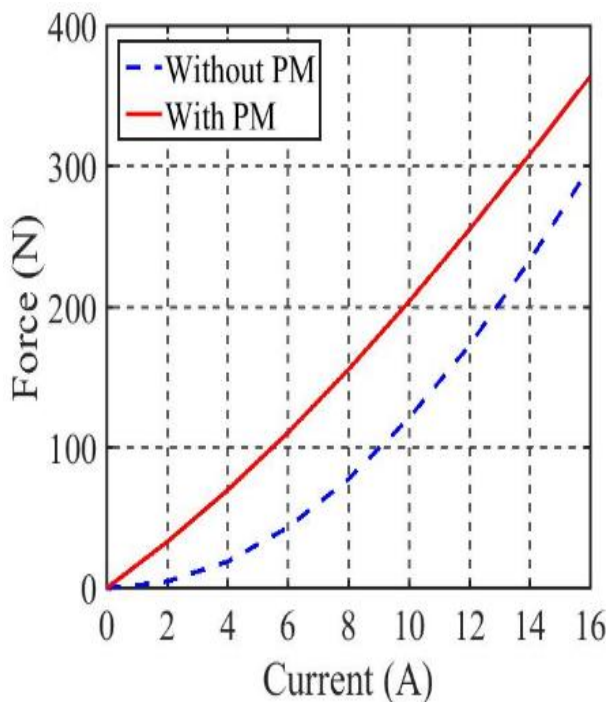


Fig. 16: Average static force for STLSRM and STPMLSRM.

This comparison shows that in all currents, the average static force has been increased by adding the PM in STLSRM structure. The dynamic characteristics of STLSRM and STPMLSRM, including instantaneous current and instantaneous thrust force, for the working point: speed = 4 m/s, turn-on position = 15.8 (mm), turn-off position = 28.3 (mm) and the current regulation control mode when maximum current is 7 A, are predicted and compared in Fig. 17.

The average instantaneous thrust force for STPMLSRM and conventional STLSRM are 82.26 N and 46.32 N, respectively, while, the effective current for STPMLSRM and conventional STLSRM are 4.41 A and 4.51 A, respectively. Therefore, adding the PM, increases the flux density in air-gap and the force applied to the translator. Using the dynamic characteristic of instantaneous thrust force (Fig. 17), the average instantaneous power for STPMLSRM and STLSRM are 329.04 W and 185.28 W, respectively, which shows that the average power for STPMLSRM is more than STLSRM.

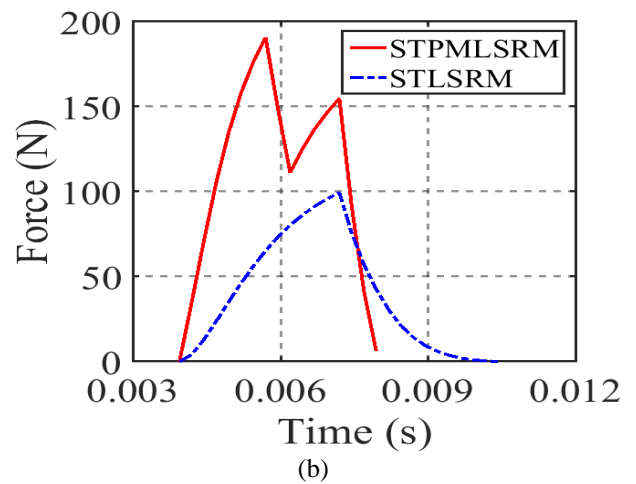
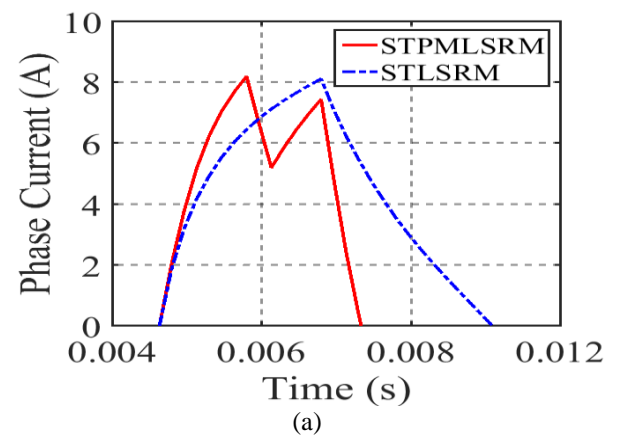


Fig. 17: 3-D Dynamic characteristics: (a) Waveform of instantaneous phase current, (b) Waveform of instantaneous thrust force.

4. CONCLUSION

In this paper, a new type of segmental translator linear switched reluctance motor was introduced, and the performance characteristics were improved by placing permanent magnets in its structure, because, the presence of the permanent magnet has a significant effect on the air-gap flux density and increases the force applied to the moving part. The right position to place permanent magnets in the segmental translator linear switched reluctance motor is the

stator yoke, because it completely covers the flux passing surface and also strengthens the magnetic flux. To validate the introduced structure, based on the finite element method, comparisons were made between the introduced motors and their static and dynamic characteristics were compared. These comparisons showed that using discrete segments instead of continuous poles in the translator and placing permanent magnets in a suitable position in the motor structure improve the motor performance. Therefore, the average static force in different currents for the segmental translator permanent magnet linear switched reluctance motor is more than the segmental translator linear switched reluctance motor. The average instantaneous thrust force for STPMSRM and conventional STLSRM were 98.45 and 49.94 N, respectively, while, the effective current for STPMSRM and conventional STLSRM were 6.3 and 5.66 A, respectively. These comparisons clearly showed that adding the permanent magnet in the motor structure, increases the flux density in air-gap and the force applied to the translator.

CREDIT AUTHORSHIP CONTRIBUTION STATEMENT

Milad Golzarzadeh: Conceptualization, Data curation, Formal analysis, Investigation, Methodology, Project administration, Resources, Software, Validation, Roles/Writing - original draft, Writing - review & editing. **Hashem Oraee:** Conceptualization, Data curation, Methodology, Project administration, Validation, Roles/Writing - original draft, Writing - review & editing. **Babak Ganji:** Conceptualization, Data curation, Methodology, Project administration, Resources, Validation, Roles/Writing - original draft, Writing - review & editing.

DECLARATION OF COMPETING INTEREST

The authors declare that they have no known competing financial interests or personal relationships that could have appeared to influence the work reported in this paper. The ethical issues; including plagiarism, informed consent, misconduct, data fabrication and/or falsification, double publication and/or submission, redundancy has been completely observed by the authors. This paper is an extension of the authors' previous work [23] which was presented in the 2024 4th National Conference on Applied Research in Electrical Engineering (AREE2024), and selected as a top paper to be printed in this journal with some extensions.

REFERENCES

- [1] P. Upadhyay, and R. K., "Design of two-phase 4/6 switched reluctance motor for bidirectional starting in washing machine application," *IEEE Trans. Ind. App.*, vol. 59, pp. 1519-1529, 2023.
- [2] X. Sun et al., "Multiobjective and multiphysics design optimization of a switched reluctance motor for electric vehicle applications," *IEEE Trans. Energy Convers.* vol. 36, pp. 3294-3304, 2021.
- [3] P. Kumar, M. Israyelu, and S. Sashidhar, "A simple four-phase switched reluctance motor drive for ceiling fan applications," *IEEE Access*, vol. 11, pp. 7021-7030, 2023.
- [4] R. Nie et al. "Comparative researches on double-sided switched reluctance linear machines with different winding connections," *IET Electr. Power Appl.*, vol. 14, pp. 2082-2091, 2020.
- [5] D. Wang et al., "Comparative analysis of different topologies of linear switched reluctance motor with segmented secondary for vertical actuation systems," *IEEE Trans. Energy Convers.*, vol. 36, pp. 2634-2645, 2021.
- [6] H. Cheng, S. Liao, and W. Yan, "Development and performance analysis of segmented-double-stator switched reluctance machine," *IEEE Trans. Ind. Electron.*, vol. 69, pp. 1298-1309, 2022.
- [7] M. Lu, and R. Cao, "Comparative investigation of high temperature superconducting linear flux-switching motor and high temperature superconducting linear switched reluctance motor for urban railway transit," *IEEE Trans. Appl. Supercond.*, vol. 31, pp. 1-5, 2021.
- [8] S. Masoudi, H. Mehrjerdi, and A. Ghorbani, "New elevator system constructed by multi-translator linear switched reluctance motor with enhanced motion quality," *IET Electr. Power Appl.* vol. 14, pp. 1692-1701, 2020.
- [9] Z. Li et al., "Nonlinear analytical model of linear switched reluctance motor with segmented secondary considering iron saturation and end effect," *IEEE Access*, 11, pp. 132078-132087, 2023.
- [10] R. Nie et al., "Compensation analysis of longitudinal end effect in three-phase switched reluctance linear machines," *IET Electr. Power App.*, vol. 14, pp. 165-174, 2020.
- [11] D. Wang, X. Wang, and X. Du, "Design and comparison of a high force density dual-side linear switched reluctance motor for long rail propulsion application with low cost," *IEEE Trans. on Mag.*, vol. 53, pp. 1-4, 2017.
- [12] W. Sun, Q. Li, L. Sun, and L. Li, "Development and investigation of novel axial-field dual-rotor segmented switched reluctance machine," *IEEE Trans. Transport. Electrification*, vol. 7, pp. 754-765, 2021.
- [13] R. Madhavan, and B. G. Fernandes, "Axial flux segmented SRM with a higher number of rotor segments for electric vehicles", *IEEE Trans. Energy Convers.*, vol. 28, pp. 203-213, 2013.
- [14] R. Vandana, and B. G. Fernandes, "Design methodology for high-performance segmented rotor switched reluctance motors," *IEEE Trans. Energy Convers.*, vol. 30, pp. 11-21, 2015.
- [15] B. Ganji, and M. H. Askari, "Analysis and modeling of different topologies for linear switched reluctance motor using finite element method," *Alexandria Engineering Journal*, vol. 55, pp. 2531-2538, 2016.
- [16] M. Golzarzadeh, and B. Ganji, "Analytical modelling of the linear switched reluctance motor with segmental translator," *IET Electr. Power Appl.*, vol. 13, pp. 527-537, 2019.
- [17] M. Golzarzadeh, H. Oraee, and B. Ganji, "Lumped parameter thermal model for segmental translator linear switched reluctance motor," *IET Electr. Power Appl.* vol. 17, pp. 1548-1561, 2023.
- [18] M. A. J. Kondelaji, E. F. Farahani, and M. Mirsalim, "Performance analysis of a new switched reluctance motor with two sets of embedded permanent magnets," *IEEE Trans. Energy Convers.*, vol. 35, pp. 818-827, 2020.

- [19] M. Masoumi, and M. Mirsalim, "E-core hybrid reluctance motor with permanent magnets inside stator common poles," *IEEE Trans. Energy Convers.*, vol. 33, pp. 826–833, 2018.
- [20] M. M. Bouiabadi, A. D. Aliabad, S. M. Mousavi, and E. Amiri, "Design and analysis of e-core PM-assisted switched reluctance motor," *IET Electr. Power Appl.*, vol. 14, pp. 859–864, 2020.
- [21] R. Cao, E. Su, and M. Lu, "Comparative study of permanent magnet assisted linear switched reluctance motor and linear flux switching permanent magnet motor for railway transportation," *IEEE Trans. Appl. Supercond.*, vol. 30, pp. 1–5, 2020.
- [22] A. Ghaffarpour, M. Vatani, M. A. Jalali, and M. Mirsalim, "Analysis of linear permanent magnet switched reluctance motors with modular and segmental movers," *IET Electr. Power Appl.* vol. 17, pp. 756–772, 2023.
- [23] M. Golzarzadeh, H. Oraee, and B. Ganji, "Modeling and comparison of various structures for linear switched reluctance motor," in *4th Conference on Applied Research in Electrical Engineering*, Ahvaz, Iran, 2024.

BIOGRAPHY



Milad Golzarzadeh is currently a PhD candidate in electrical power engineering at Sharif University of Technology, Tehran, Iran. His research interests include modeling and design of electric machines, linear switched reluctance motors, thermal modeling of electric machines, permanent magnet motors and power electronics.



Hashem Oraee (Fellow of IET, Senior Member of IEEE) received the B.Eng. in electrical and electronic engineering from University of Wales, Cardiff, U.K., in 1980, and the Ph.D. degree in electrical machines from the University of Cambridge, Cambridge, U.K., in 1984. He is currently a Full Professor with the Department of Electrical Engineering, Sharif University of Technology, Tehran, Iran. His current research interests include renewable energies, electrical machines, and DFIGs.



Babak Ganji (Senior Member of IEEE) received the B.Sc. degree from Esfahan University of Technology, Iran in 2000, and M.Sc. and Ph.D. from the University of Tehran, Iran in 2002 and 2009 respectively, all in electrical power engineering. He is currently an Associate Professor with the Faculty of Electrical and Computer Engineering, University of Kashan, Kashan, Iran. His research interest is modeling and design of advanced electric machines, especially switched reluctance motor.

Copyrights

© 2025 Licensee Shahid Chamran University of Ahvaz, Ahvaz, Iran. This article is an open-access article distributed under the terms and conditions of the Creative Commons Attribution –NonCommercial 4.0 International (CC BY-NC 4.0) License (<http://creativecommons.org/licenses/by-nc/4.0/>).

